JOURNAL OF MATERIALS SCIENCE 5 (1970) 1063-1072

The Recovery Creep of Niobium-stabilised Austenitic Stainless Steels

K. R. WILLIAMS, I. R. McLAUCHLIN
Central Electricity Generating Board, Berkeley Nuclear Laboratories, Berkeley, Gloucester, UK

The creep properties of niobium-stabilised stainless steels of carbon contents in the range 0.01 to 0.05% carbon can be accounted for by the general recovery theory of creep. The high stress dependencies of recovery and creep rate can be adequately explained through an internal friction stress or impedance term, retarding recovery. Measurement of this friction term by dislocation density and stress relaxation techniques provides the correct stress dependencies when applied to the modified recovery theory.

1. Introduction

The recovery theory of creep is based on the knowledge that metals harden with strain, and soften with time on heating [1, 2]. During steady state creep, it was postulated that there will be an exact balance between strain-hardening and recovery, such that the steady state creep rate is given by

$$\dot{\epsilon}_s = \frac{r}{h} \tag{1}$$

where r $(= -\partial\sigma/\partial t)$ is the rate of recovery and h $(= \partial\sigma/\partial\epsilon)$ is the strain-hardening coefficient. Work by Cottrell and Aytekin [3] provided some confirmation of this relation. The theory has recently acquired added importance due to the theoretical and experimental work of McLean *et al* [4-7] who have shown that the above relation is a general one and holds for pure metals and single phase alloys. More recent work on these materials has shown that the theory can be extended into the primary and tertiary stages of creep with equal success [8-11].

The theories of McLean *et al* [4-7] although very attractive due to their inherent simplicity, are not generally applicable to high-strength particle-hardened material. In general they suffer from an inability to predict the high stress dependence of the recovery and creep rates found in such materials, although McLean [7] has shown in principle the way in which this discrepancy arises. In addition, it has been found difficult to test the recovery theory on materials containing second phase particles, as it is often not easy and sometimes impossible [12] to measure a value for the work hardening coefficient of creep tested specimens.

McLean's theories [4-7] assume that the dislocations formed during creep exist in a three-dimensional network, and that the growth of such a network, essentially by climb of dislocations, constitutes the recovery process. If the average mesh size of the network is x, the driving force for recovery is inversely proportional to x [13] and the growth rate of the average network size is given by

$$\frac{dx}{dt} = \frac{M \cdot T_D}{x} \tag{2}$$

where M = mobility factor and T_D = line tension of the dislocation.

This treatment is analogous to that applied to normal grain growth, and the influence of particles in retarding the growth rate [14] can be applied in a similar manner. Lagneborg [15] has introduced an impedance factor, Z, into equation 2 such that Z depends both on the number and size of the impeding particles, and on the nature of the particle-dislocation interaction. A growing network will thus experience a retarding force denoted by T_DZ, and equation 2 then becomes

$$\frac{dx}{dt} = \frac{MT_D}{2}\left(\frac{1}{x} - Z\right)^2. \tag{3}$$

Since it is well established that $\sigma \propto$ (dislocation density, $\rho)^{\frac{1}{2}}$ [4, 16] and $x \propto \rho^{-\frac{1}{2}}$, then equation 3 becomes

$$r = \frac{d\sigma}{dt} = \frac{MT_D\sigma}{2}\left(\frac{\sigma}{\alpha\mu b} - Z\right)^2 \tag{4}$$

where α = proportionality constant ~ 1, μ = shear modulus, and $\mathbf{b}$ = Burgers vector.

It has been shown [15] that the stress dependence of both the creep and recovery rates can vary between wide limits depending on the value of Z chosen. It thus appears that this modified recovery theory can account for the creep behaviour of particle-hardened material, providing that Z is given an appropriate value. Lagneborg [15] has related Z to the positive stress intercept on a plot of creep stress against $\mu\mathbf{b}\sqrt{\rho}$, but is rather vague as to the physical nature of this parameter.

The purpose of this report is to describe an investigation into the high temperature creep and recovery properties of a series of 20% Cr, 25% Ni, 1% Nb, stainless steels with carbon content in the range 0.01 to 0.05% to produce varying volume fractions of particles in the form of NbC. The creep results obtained have been related to results of stress relaxation carried out during hot tensile tests, and to dislocation density counts from thin foil electron microscopy.

It is found that the various techniques employed yield complementary results and enable a more meaningful description of the impedance factor Z, and its relation to the recovery theory to be advanced.

2. Experimental Procedure

The chemical compositions of the steels used are listed in table I. Specimens of 2.54 cm gauge length, 0.64 cm wide were stamped from 0.064 cm thick sheet obtained from cold worked AGR reactor fuel cladding material. These were annealed in a vacuum for 30 min at 930°C to produce a recrystallised structure of grain size 20 μm, containing spherical NbC precipitates.

Creep tests were carried out at 750°C in a vacuum of $\sim 10^{-5}$ torr using a conventional constant load creep machine. All creep strains were small so that conditions approximated to those of constant stress. The specimen strain was measured to an accuracy of 3×10^{-5} cm using a dial gauge. The temperature was controlled to $\pm$ 1°C with less than 1°C temperature gradient over the specimen gauge length. All tests were allowed 2 h to reach an equilibrium temperature before applying the load.

Recovery measurements were made by rapidly removing $\sim$ 10% of the applied load ($\Delta\sigma$) and noting the induction period (Δt) before creep recommenced. The recovery rate is then given by

$$r = \frac{-\partial\sigma}{\partial t} = -\left(\frac{\Delta\sigma}{\Delta t}\right)_{\Delta\sigma\to 0} \tag{5}$$

The associated work hardening coefficient (h) was measured by noting the instantaneous extension ($\Delta\epsilon$) on re-application of the stress increment $\Delta\sigma$ such that

$$h = \frac{\partial\sigma}{\partial\epsilon} = \frac{\Delta\sigma}{\Delta\epsilon} \tag{6}$$

This procedure was not entirely satisfactory since it was impossible to determine the end of the $\Delta\epsilon$ period accurately using the dial gauge. For this reason it was found to be more reliable to determine h from flow stress measurements made on creep tested specimens. These were obtained using a modified Instron machine at room temperature and at strain rates comparable with those measured during the creep test. The tangent to the flow stress curve at the creep stress (corrected for the change in modulus with temperature), gives a measure of h.

Stress relaxation curves were obtained at 750°C using a hard Instron tensile machine. Calibration experiments indicated that plastic relaxation of the machine was negligible over the time periods and stress ranges of specimen relaxation. Strain rates in the range 3.33×10^{-3} to 3.33×10^{-5} sec^{-1} were used during these tests. The basic relaxation measurement was made by arresting the Instron cross head and recording the decrease in load with time. A typical relaxation curve is shown in fig. 1, in which it is seen that the residual stress (σ_i) decreases smoothly from the initial value σ_A to a pleateau at σ_i. Stress cycling techniques [17, 18] were employed to show that the same relaxation curve was followed even if the initial σ_A was abruptly reduced to a lower value above σ_i. Also

TABLE I Chemical composition (wt %) of steels

Designation	C	Cr	Ni	Nb	Si	Mn	S	P	B	Co
0.01C	0.008	20.4	25.5	0.6	0.68	0.65	0.02	0.01	2 ppm	50 ppm
0.05C	0.049	20.9	24.7	0.6	0.59	0.64	0.02	0.01	2 ppm	50 ppm

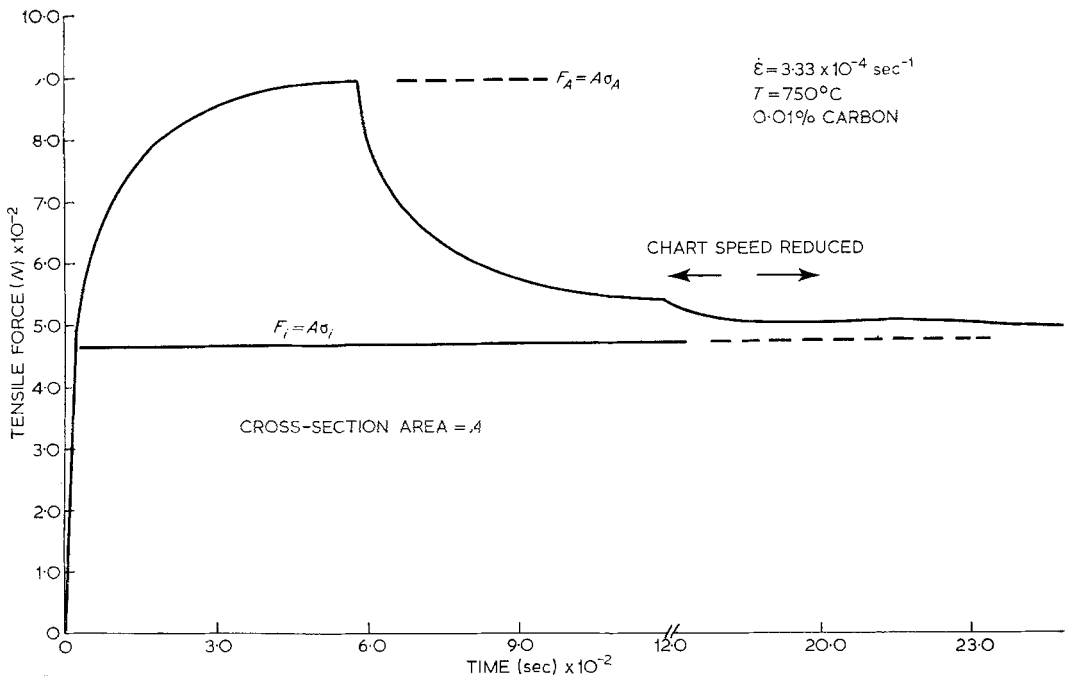

Figure 1 Diagrammatic plot showing creep and stress relaxation.

rapid reductions in applied stress to a value below σ_i were followed by an initial stress rise (fig. 2).

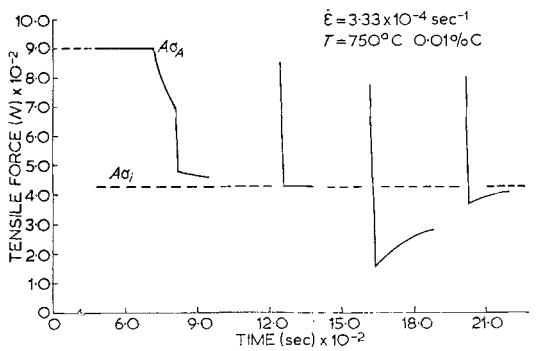

Figure 2 Stress reduction experiments near the internal stress.

Dislocation densities (ρ) were counted on foils from specimens crept into the secondary stage and cooled rapidly ($\sim$ 100°C/min) under load. The line intercept method [19] was used, so that

$$\rho = \frac{2N}{Lt} \tag{7}$$

where N = number of intercepts, t = thickness of foil (obtained from slip trace measurements), and L = projected length of line. Thin foils were prepared from deformed specimens using an initial chemical thinning solution [20] containing 50% HCl, 10% HNO_3, 5% H_3PO_4 and 35% H_2O at 80°C. This was followed by the conventional window method using a 60% H_3PO_4, 40% H_2SO_4 electrolyte at 60°C and 9 V. Electron micrographs were obtained using a Philips EM 200 microscope incorporating a $\pm$ 20° tilting device. This enabled multiple diffraction conditions to be established, so that the maximum number of dislocations was counted.

3. Results

The steady state creep rates obtained during both creep and tensile tests are plotted against stress on a log-log basis in fig. 3. The stress exponent varies between 5.5 and 6.5 (depending on carbon level), over the majority of the stress range, but deviations exist at the high and low stress extremes. At a given stress the lower carbon alloy creeps at a slower rate than the higher carbon steel.

The recovery rate shows a similar stress dependence over the same stress range (fig. 4). Work hardening coefficients, obtained from

TABLE II Creep test data

A Temperature constant at 750°C Stress MN/m^2	Measured strain rate sec^{-1}	Recovery rate (r) $MN/m^2/sec$	Work hardening coefficient (h) MN/m^2	Calculated strain rate $\dot{\epsilon}_s$ ($= r/h$) sec^{-1}	Activation volume (v) m^3
128.4	2.59×10^{-5}	1.01×10^{0}	2.76×10^{4}	3.73×10^{-5}	1.5×10^{-27}
111.0	7.83×10^{-6}	4.22×10^{-1}	4.73×10^{4}	8.98×10^{-6}	1.5×10^{-27}
103.4	7.32×10^{-6}	1.84×10^{-1}	1.73×10^{4}	1.06×10^{-5}	1.6×10^{-27}
79.4	1.12×10^{-6}	2.45×10^{-2}	2.96×10^{4}	8.18×10^{-7}	1.8×10^{-27}
60.5	1.59×10^{-7}	4.2×10^{-3}	4.03×10^{4}	1.043×10^{-7}	2.1×10^{-27}
B Stress constant at 128.4 MN/m^2 **Temperature (°C)**					
730	7.88×10^{-6}	4.61×10^{-1}	4.73×10^{4}	9.66×10^{-6}	1.0×10^{-27}
710	2.86×10^{-6}	1.84×10^{-1}	3.66×10^{4}	4.82×10^{-6}	0.90×10^{-27}
690	8.90×10^{-7}	2.59×10^{-2}	3.52×10^{4}	7.37×10^{-7}	2.1×10^{-27}

$1 MN/m^2 = 10^{-1}$h bar

creep and tensile tests, appear to be independent of stress and are given in table II.

Substitution of the measured values of r and h into equation 1 produces values of $\dot{\epsilon}_s$ in good agreement with the values measured experimentally, as shown in table II.

The activation volume (v) was obtained from the stress reduction tests made during recovery measurements [6],

$$v \cdot \Delta\sigma = kT \ln \dot{\epsilon}_1/\dot{\epsilon}_2 \quad (8)$$

where $\Delta\sigma$ = stress decrease, $\dot{\epsilon}_1$, $\dot{\epsilon}_2$ = creep rates before and after the stress reduction, and k, T have their usual meaning. Values of v obtained from this equation are given in table II.

Dislocation densities are plotted against stress

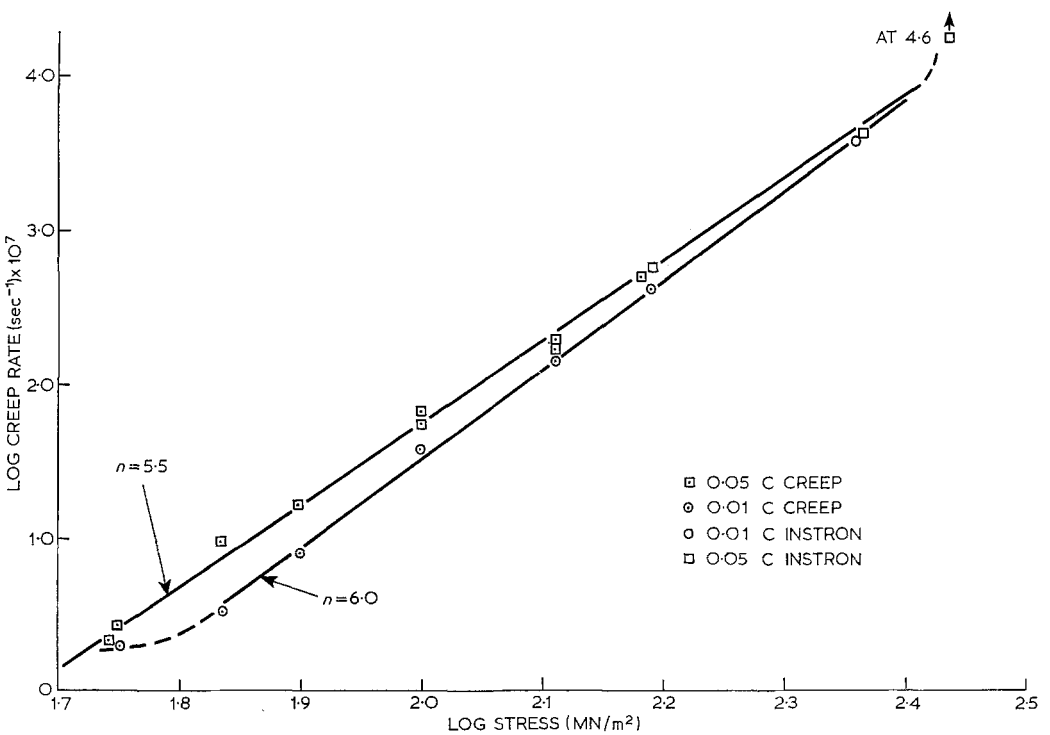

Figure 3 Observed stress dependence of creep rate.

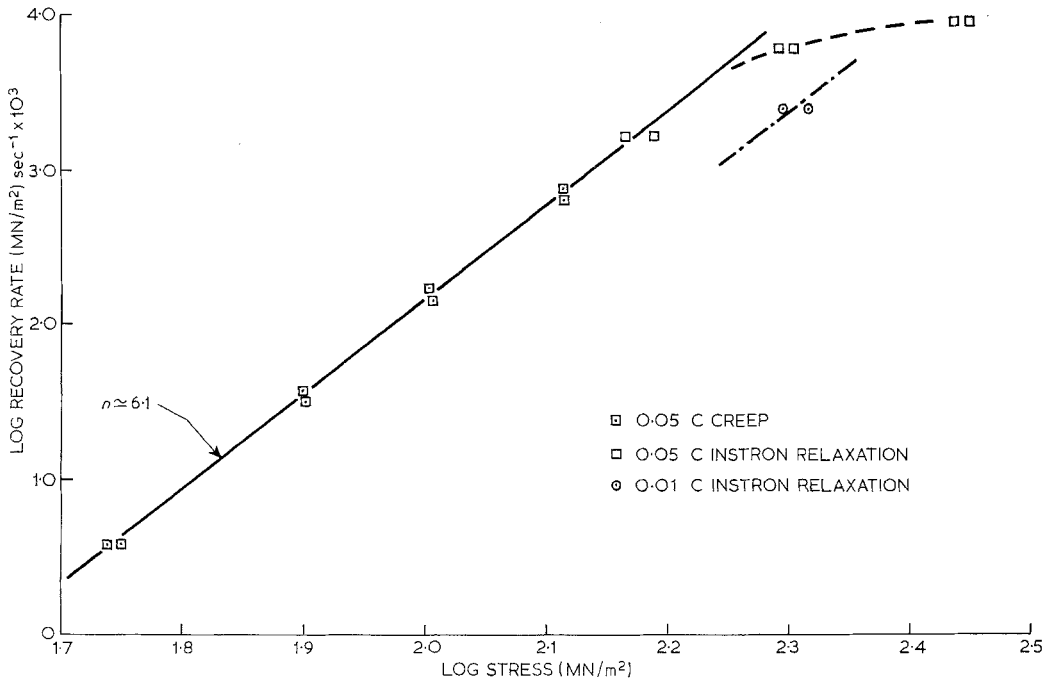

Figure 4 Observed stress dependence of recovery rate.

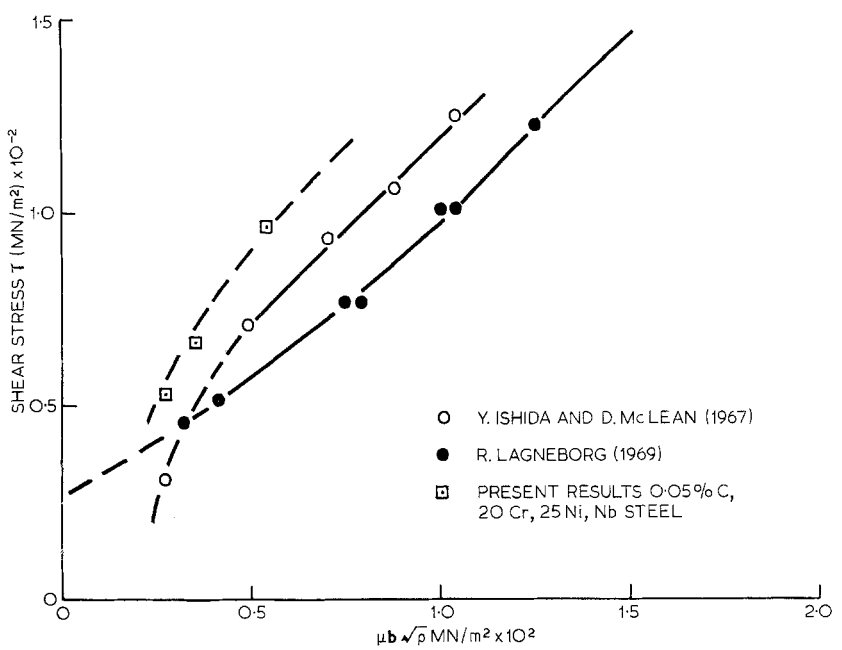

Figure 5 Creep stress τ ($= \sigma/2$) *vs.* $\mu b\sqrt{\rho}$ for impure iron (Ishida and McLean), stainless steel (Lagneborg) and present results.

in fig. 5. Also shown are results of Lagneborg [21] for a 20% Cr, 35% Ni stainless steel and Ishida and McLean [6] for an Fe-Mn-N alloy. The points can be fitted to the following relation over part of the stress range:

$$\sigma = \sigma_0 + \alpha\mu b\sqrt{\rho} \qquad (9)$$

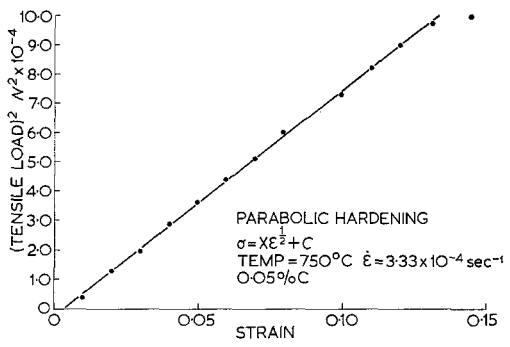

Figure 6 Parabolic hardening during tensile flow.

where σ_0 = intercept on stress axis = friction stress and α = constant ~ 1.0.

The hot tensile results followed the normal parabolic work hardening law, as shown for a typical test in fig. 6, i.e.

$$\sigma = \chi\epsilon^{\frac{1}{2}} + C \; . \qquad (10)$$

However, restraining after relaxation resulted in a different flow curve, independent of the time of recovery. This is shown diagrammatically in fig. 7. Differentiating (10) gives

$$h = \frac{\partial\sigma}{\partial\epsilon} = \frac{\chi}{2\epsilon^{\frac{1}{2}}} \qquad (11)$$

with $\chi = 2.02 \times 10^2$ MN/m² from fig. 6.

Equation 11 gave a value for the initial work hardening coefficient of the annealed material, $h_i = 1.5 \times 10^3$ MN/m², for an initial extension of 0.5% compared with values measured on restraining the hardened material of $h_a = h_b = 3.45 \times 10^4$ MN/m². Such behaviour is analogous to that observed during primary creep [10, 11] in which h increases by approximately an order of magnitude early in the creep test.

Analysis of the relaxation curves obtained during the tensile tests showed that an empirical relationship of log (residual stress, σ_t) against log (time) gave a good straight line over a wide stress range between σ_A and σ_i. Such a plot is shown in fig. 8 in which it can be seen that

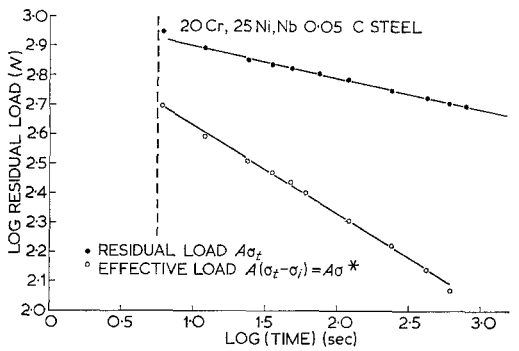

Figure 8 Log (residual load) *vs.* log (time) for isothermal relaxation.

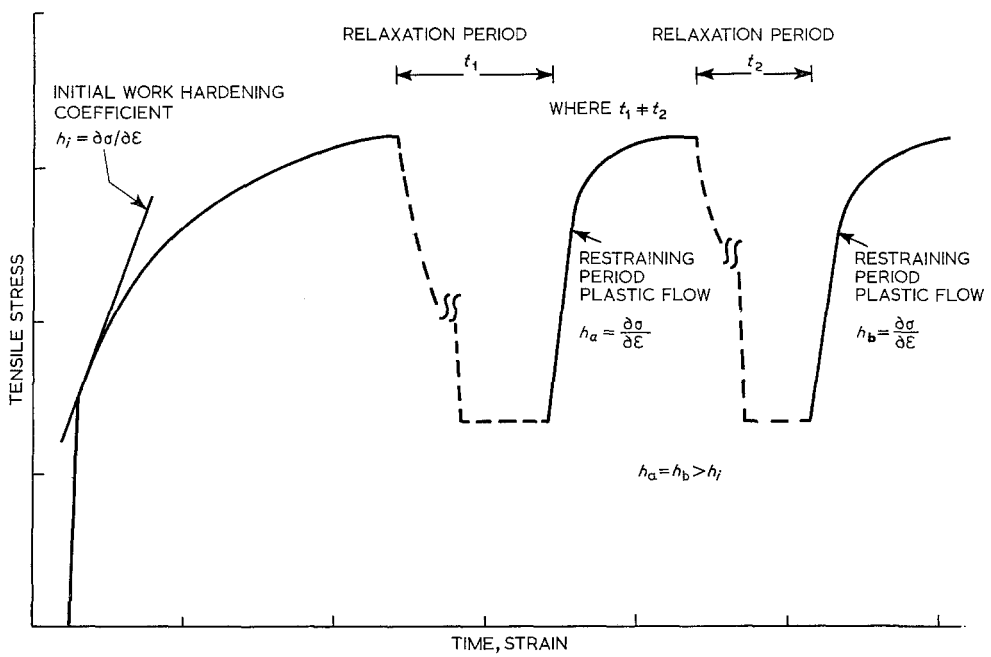

Figure 7 Diagrammatic flow stress curve, showing two periods of relaxation followed by further strain.

TABLE III Stress relaxation data at 750°C together with friction stress values

Strain rate $\dot{\epsilon}$ sec^{-1}	Carbon content wt %	σ ultimate flow stress MN/m^2	σ_y yield stress MN/m^2	σ_i internal stress MN/m^2	σ_0 friction stress MN/m^2
3.33×10^{-3}	0.05	278.8	98.4	94.7	90.0
3.33×10^{-4}	0.05	231.2	94.2	89.9	70.0
3.33×10^{-5}	0.05	151.8	75.2	70.2	60.0
3.33×10^{-4}	0.01	231.2	104.4	99.8	70.0

$$\log \sigma = m' \log t + \gamma \qquad (12)$$

where $m' = -0.12$.

On the same figure is plotted the effective residual stress, i.e. $(\sigma_t - \sigma_i)$, which fits a similar linear equation with $m' = -0.33$. Measured values of σ_i are collected in table III together with the ultimate flow stress, macroscopic yield stress and strain rate. Also given are estimates of the friction stress, σ_0, from fig. 5 which show the same trends as σ_y and σ_i.

4. Discussion

Reference to fig. 3 shows that the creep results are of the general form found for this type of stainless steel [15, 22]. Over the majority of the stress range, the results can be fitted to a power law dependence, i.e.

$$\dot{\epsilon} = A \sigma^n f(T) \qquad (13)$$

where $f(T)$ = temperature function, A = constant, and n varies between 5.5 and 6.5.

On this graph are also plotted the ultimate flow stresses for corresponding strain rates obtained from tensile tests. Clearly these results fall on an extrapolated log $\dot{\epsilon}_s$ against log σ data line, so that it can be assumed that similar rate controlling processes are in operation. This statement takes on a greater significance when comparisons are made of the stress dependence of the recovery rate from separate creep tests, with that obtained from stress relaxation.

During stress relaxation, it has been shown [17, 23] that elastic strain in the specimen and machine is gradually replaced by plastic strain in the specimen according to

$$-\frac{1}{E^*} \cdot \frac{d\sigma}{dt} = \dot{\epsilon} \qquad (14)$$

where E^* is the effective modulus of machine and specimen.

From equation 12 and fig. 8 we have

$$\sigma = \gamma t^{m'}$$

with m' negative and fractional.

Let

$$m' = \frac{-1}{\theta} .$$

Then

$$\sigma = \gamma t^{-1/\theta}$$
$$t = \gamma' \sigma^{-\theta}$$

and

$$\frac{d\sigma}{dt} = \gamma'' \sigma^{\theta+1} . \qquad (15)$$

Substituting equation 15 into equation 14 we have

$$\dot{\epsilon} = A' \sigma^{\theta+1} = r/h$$
$$\therefore r = A' h \sigma^{\theta+1}$$

h, in the present tests, appears to be independent of stress, while γ and hence A' would have the usual Arrhenius temperature dependence. Thus we have during relaxation

$$r = A_1 \sigma^{\theta+1} f(T) . \qquad (16)$$

During stress relaxation, only part of the flow stress is recoverable, and the curves tend to a limiting stress value σ_i, the internal stress. Thus considering the network growth model of creep [4-7], the dislocation network is recovering not under the applied stress but under an effective stress

$$\sigma^* = \sigma_t - \sigma_i \qquad (17)$$

which will necessarily alter the stress dependence of the creep parameters. Inserting the value of $m' = -0.33$, associated with the effective stress σ^*, into equation 16 gives

$$r = A_1 \sigma^4 f(T) \qquad (18)$$

The use of σ_i as a modifying factor impeding recovery thus produces a stress exponent for recovery rate in particle hardened material equal to that required by the recovery theories of creep for single phase alloys.

The unmodified plot in fig. 8 would be expected to give a higher exponent than 4, approxi-

mating the exponents found from the creep work. Using $m' = -0.12$, associated with the residual stress during relaxation, σ_i, we have

$$r = A_2 \sigma^9 f(T) . \quad (19)$$

This derivation does give an increased stress exponent, but the value is higher than that observed from creep tests (see fig. 4). However, the relaxation data was obtained within a higher stress range than that employed for creep. Since σ_i increases with increasing stress, the values of σ_i in fig. 8 are higher than those which would be given by relaxation in the creep stress range. While this does not affect equation 18, it does give a stress exponent in equation 19 which is slightly high.

From table III it will be seen that the macroscopic yield stress $\sigma_y \simeq \sigma_i$. It has been shown that σ_i can account for the increased stress dependence shown during creep of material hardened by a second phase. If the above equality is typical for metallic systems of the present type, a more clearly understood physical meaning can be given to the impeding term in the present investigation (Lagneborg's Z) and the factors that govern the yield point directly influence the recovery rate and its stress dependence. For the present material the largest influence on the yield point is likely to come from particle pinning of dislocations. The NbC precipitates exist in a bimodal distribution with a separation of the smaller particles of $\Lambda \simeq 10^{-5}$ cm. Thus the flow stress according to the Orowan relation

$$\sigma = \frac{2\mu\mathbf{b}}{\Lambda} \quad (20)$$

is that required to bend dislocations to a radius of $\Lambda/2$. Substituting the present value of Λ into equation 20 gives a macroscopic flow stress of approximately 70 to 100 MN/m² which is in good agreement with the observed values of σ_y. It would therefore appear from such an argument that the rate of recovery of the dislocation network is limited by its inability to bow between the incoherent particles existing in the lattice. Activation volume measurements (table II) confirm that the inter-particle length of dislocation is of the order 10^{-5} cm, thus

$$v = l \,.\, \mathbf{b} \,.\, d \quad (21)$$

where l = activated length between particles, $\mathbf{b}$ = Burger's vector, and d = activation distance.

For a climb mechanism of recovery, d would be expected to be of the order of 1 Burger's vector. Substituting typical values in this equation gives

$$10^{-27} = l \times \mathbf{b}^2$$
$$= l \times 10^{-20}$$

and

$$l = 10^{-7} \text{ m or } 10^{-5} \text{ cm} .$$

The nearer σ_y approaches the ultimate flow stress (i.e. the smaller is σ^*), the slower is the recovery rate and hence the higher the stress dependence. From table III it is evident that for a given ultimate flow stress, a decrease in carbon content gives an increase in σ_y, which is expected for non-coherent particle hardening [24]. From the preceding discussion it would follow that a decrease in carbon content would thus result in an increase in the stress dependence and a decrease in creep rate, and hence recovery rate. The present results confirm this. For a given applied stress, the effective stress, σ^*, acting on the dislocation network is decreasing with decreasing carbon content. However, $\sigma^* \propto 1/x \propto \mathrm{d}x/\mathrm{d}t$ and so the driving force for recovery is also decreasing. Thus at smaller carbon contents recovery is slower and better creep resistance is to be expected.

The present work has indicated that both σ_i and σ_y can be equated with the impedance factor, Z, employed by Lagneborg [15] in equation 4 as a modification to the creep recovery theories. Lagneborg has attempted to clarify Z by putting

$$Z \simeq \frac{\sigma_0}{\alpha\mu\mathbf{b}} \quad (22)$$

so that

$$r = \frac{MT_D\sigma}{2}\left(\frac{\sigma}{\alpha\mu\mathbf{b}} - \frac{\sigma_0}{\alpha\mu\mathbf{b}}\right)^2 . \quad (23)$$

The plot of σ against $(\rho)^{\frac{1}{2}}$ (fig. 5) for the present material appears to show a non-linear dependence at lower stresses similar to that found by Barrett and Nix [25] and Ishida and McLean [6]. Thus a value of σ_0 at any stress can only be obtained by drawing a tangent to the curve and extrapolating to obtain the positive stress intercept. Clearly, the higher the stress the higher the value of σ_0 obtained in this way, which again indicates why the stress exponent in equation 19 is too high.

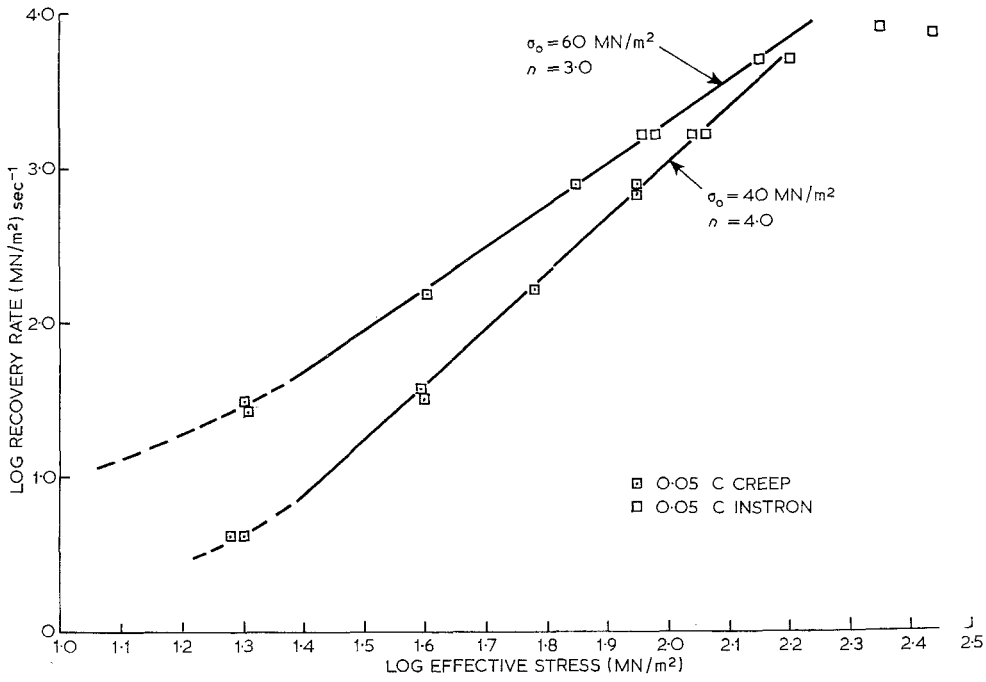

Figure 9 Corrected stress dependence of recovery rate.

Estimated values of σ_0 compare quite well with σ_i and σ_y in table III. Thus we can say that the impedance term

$$Z \simeq \sigma_i = \sigma_y = \sigma_0 \qquad (24)$$

Fig. 9 shows that the stress dependence of recovery rate is reduced from 6.1 to 4.0 by introducing a Z term equal to 40 MN/m^2, and to 3.0 when Z equals 60 MN/m^2.

It is evident that equation 4, and hence equation 23, cannot apply at values of Z greater than the applied stress, but as mentioned above, it is unlikely that σ_0, and therefore Z, remain constant with stress. In the low stress regime, diffusion can help in decreasing the effectiveness of dislocation obstacles so that σ_0 would be expected to decrease. In this context, therefore, we have taken σ_0 to be a friction stress, i.e. the dislocations are impeded on moving in the lattice.

An estimate of the friction stress can be obtained on McLean's network model. Fig. 10 shows the usual distribution function of individual link flow stresses [7]. σ_1 is then the resistance to glide from the dislocation elastic forces only, while σ_2 is the applied stress necessary if there are other resistances equal to $(\sigma_2 - \sigma_1)$. Since the creep rate is usually expressed as

$$\dot{\epsilon} \propto {\sigma_2}^p$$

then

$$\dot{\epsilon} = \propto \sigma^{\frac{n}{1}} = \beta\sigma^{\frac{\rho}{2}}$$

and

$$\frac{\mathrm{d} \ln \dot{\epsilon}}{\partial\sigma} = \frac{n}{\sigma_1} = \frac{p}{\sigma_2}$$

or

$$\sigma_1 = \frac{n}{p}\sigma_2 \ .$$

For the present results $p = 6$, and taking n as the theoretical value 4.5 predicted by the unmodified recovery theory, then for an applied creep stress of $\sigma_2 = 140$ MN/m^2

$$\sigma_1 = 105 \text{ MN/m}^2$$

and

$$\sigma_0 = (\sigma_2 - \sigma_1) = 35 \text{ MN/m}^2 \ .$$

This is near to the Z value chosen to give the correct stress dependence of recovery rate. Clearly, if on increasing the applied stress σ_2, σ_1 increases by the same amount then σ_0 is a constant as is sometimes found [6, 15]. However, for the present series of tests it would appear that σ_0 is decreasing with decreasing stress and σ_2 and σ_1 are not following each other linearly.

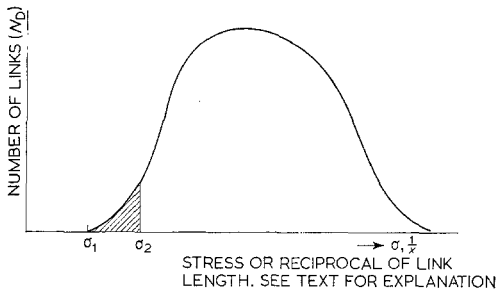

Figure 10 Distribution of number of links (N_D) in a three dimensional dislocation network, with their individual flow stresses.

The present results also demonstrate the marked stability of the network of dislocations. This is evident from fig. 7 in which the material was allowed to recover down to the internal stress and annealed at this stress for several hours. On re-straining, the material retains a much higher value of h than obtained from the initial extension (equations 10 and 11). This behaviour has been observed [26] in strain-hardened nickel.

5. Conclusions

(1) In agreement with the work of Lagneborg [15] the recovery theory of creep can be modified to take into account the effect of second phase particles, by incorporating an impedance factor (Lagneborg's Z), which retards recovery.

(2) The recovery rate is slower, and the stress-dependence of recovery rate higher, the larger the value of Z.

(3) The impedance factor Z is greater in the material containing the smaller carbon content which apparently indicates the existence of a critical carbide size and spacing for a minimum recovery rate.

(4) Both σ_i, the internal stress measured during relaxation, and σ_y, the macroscopic yield stress, can be equated with Z and give the theoretical stress dependence of recovery rate during relaxation.

(5) Values of σ_0, a friction stress, estimated from a plot of σ against $(\rho)^{\frac{1}{2}}$ are similar to σ_i and σ_y and can be used in a similar manner when plotting effective stresses.

Acknowledgement

This paper is published by permission of the Central Electricity Generating Board.

References

1. R. W. BAILEY, *J. Inst. Metals* **35** (1926) 27.
2. E. OROWAN, *J. West Scotland Iron & Steel Inst.* **54** (1946-47) 45.
3. A. H. COTTRELL and V. AYTEKIN, *J. Inst. Metals* **77** (1950) 389.
4. D. MCLEAN and K. F. HALE, Structural processes in Creep, *Iron and Steel Inst. Spec. Report* (1961) p. 19.
5. D. MCLEAN, *Reports Progr. Phys.* **29** (1966) 1.
6. Y. ISHIDA and D. MCLEAN, *J. Iron & Steel Inst.* **205** (1967) 88.
7. D. MCLEAN, *Trans. Met. Soc. AIME* **242** (1968) 1193.
8. P. W. DAVIES and K. R. WILLIAMS, *Acta Metallurgica* **17** (1969) 897.
9. *Idem, J. Inst. Metals* **97** (1969) 337.
10. W. J. EVANS and B. WILSHIRE, *Trans. Met. Soc. AIME* **242** (1968) 2514.
11. T. WATANABE and S. KARASHIMA, Paper presented at Int. Conf. on the Strength of Metals and Alloys, Tokyo, 1967.
12. D. SIDEY and B. WILSHIRE, *Metal Sci. J.* **3** (1969) 56.
13. J. FRIEDEL, "Dislocations" (Pergamon Press, London, 1964).
14. M. HILLERT, *Acta Metallurgica* **13** (1965) 227.
15. R. LAGNEBORG, *J. Mater. Sci.* **3** (1968) 596.
16. H. WEIDERSICH, *J. Metals* **16** (1964) 425.
17. G. B. GIBBS, *Phil. Mag.* **13** (1966) 317.
18. C. M. AHLQUIST and W. D. NIX, *Scripta Met.* **3** (1969) 679.
19. P. B. HIRSCH, A. HOWIE, R. B. NICHOLSON, D. W. PASHLEY, and M. J. WHELAN, "Electron Microscopy of Thin Crystals" (Butterworths, London, 1965) p. 415.
20. A. F. ROWCLIFFE, *J. Inst. Metals* **94** (1966) 263.
21. R. LAGNEBORG, *Metal Sci. J.* **3** (1969) 18.
22. B. RUSSEL, R. K. HAM, J. M. SILCOCK, and G. WILLOUGHBY, *ibid* **2** (1968) 201.
23. G. A. SARGEANT, *Acta Metallurgica* **13** (1965) 663.
24. D. HULL, "Introduction to Dislocations" (Pergamon Press 1965) p. 224.
25. C. R. BARRETT and W. D. NIX, *Acta Metallurgica* **13** (1965) 1247.
26. S. K. MITRA and D. MCLEAN, *Metal Sci. J.* **1** (1967) 192.

Received 12 June and accepted 13 September 1970.